



Vertical and Lateral Displacement Response of Foundation to Earthquake Loading

A. F. I. Al-Ameri^a, F. W. Jawad^b, M. Y. Fattah^c

^a Civil Engineering Department, College of Engineering, University of Baghdad, Iraq

^b Ministry of Higher Education and Scientific Research, Department of Reconstruction and Projects, Baghdad, Iraq

^c Building and Construction Engineering Department, University of Technology, Baghdad, Iraq

PAPER INFO

Paper history:

Received 03 April 2020

Received in revised form 15 June 2020

Accepted 04 August 2020

Keywords:

Earthquake Loading

Vertical and Lateral Displacements

Stiffness Ratio

Abaqus Program

ABSTRACT

Risks are confronting the foundations of buildings and structures when exposed to earthquakes which leads to high displacements that may cause the failure of the structures. This research elaborates numerically the effect of the earthquake on the vertical and lateral displacement of footing resting on the soil. The thickness of the footing and depth of soil layer below the footing was taken as (0.5, 1.0, and 2.0 m) and (10, 20 and 40m), respectively. The stiffness ratio of soil to footing was also elaborated at 0.68, 0.8, 1.0, and 1.7. The results showed an increase in the vertical displacement of footing as the duration of the earthquake increases. The increase of soil layer thickness below the footing leads to a reduction in the vertical and lateral displacement. While an increase in the thickness of the footing leads to a decrease in the lateral displacement of the footing meanwhile no effect was noticed in the vertical displacement. It was noticed that the time lag between the maximum vertical displacement and the highest value of the earthquake loading is about 0.27 s. It was found that as the distance between the footing and the source of earthquake load increases, the effect of damping on the earthquake load increases while the lateral displacement decreases. The results revealed that an increase in the stiffness ratio leads to a decrease in the vertical displacement and a reduction in the response of the lateral displacement till reaching the value of stiffness ration of unity.

doi: 10.5829/ije.2020.33.10a.05

NOMENCLATURE

b	Width of the footing	S	Soil factor
d	Thickness or depth of the soil layer under the footing	av	vertical ground acceleration
F	dimensionless soil inertia force	g	acceleration of gravity
Ec	Modulus of elasticity for concrete	Greek Symbols	
Es	Modulus of elasticity for soil	$\phi'd$	Design angle of the shearing resistance of soil
Nc, N γ and N γ q	Bearing capacity factors	γ_d	Dry unit weight of soil
RSM	Rubber-soil mixture	ψ	Dilation angle
t	Thickness of the footing	γ_c	Unit weight of concretet
Nmax	seismic vertical centred load		

1. INTRODUCTION

Building under seismic waves depends mainly on deformation of members and bonded of the lateral load

resisting system; while importance of deformation demand/capacity in performance-based frameworks has been defined for decades. There is still a major unbonded to this philosophy when it comes to soil foundation systems. Because current seismic design/assessment codes only go as far as recognizing the finite stiffness and the finite bearing capacity of foundation with no consideration to their deformation

*Corresponding Author Email: alameri.abbas@gmail.com
(A. F. I. Al-Ameri)

ability. The failures which have been illustrated from the past earthquakes are two types (bearing capacity failure and settlement of foundation). The building may fail upon subjected to earthquake and the building tilted up to 60° and sunk up to 3.8 m in Nigata [1]. The loading is defined as dynamic load when it changes over time in value and or direction [2].

The type of dynamic load applied to soil or foundation relies on the nature of its creator source [3]. As well as, the soil deformation may change from small amplitude (elastic) to large (plastic) during earthquake [4]. It is well known that the behaviour of soil under dynamic is different from that under static loads through the stress-strain relationship of soil and is always nonlinear behaviour.

It always needs to state earthquake loading as plastic behaviour since high deformation occurs and it is mainly depending on the power and severity of the earthquake [5].

From a structural point of view, the footing should satisfy two requirements. The first one is the factor of safety against shear failure would be more than or equal to 2 under seismic loads and the second one is the permanent soil deformation is adjusted by the footing and superstructure. Some of the empirical steps available to calculate these issues for footing types have been discussed. Common strategies adopted by geotechnical engineers in the footing design have also been briefly discussed [6].

The problem of the earthquake bearing capacity of shallow footing has been solved indirectly, either by an increase of the static allowable ground, pressures connected to the probability of occurrence of the design seismic or by adopting an equivalent pseudo-static procedure [7].

A solution was presented by Maeda et al. [8] that can be applied widely to compute bearing capacity of shallow footings subjected to both inclined loads applied of the superstructure and inclined bearing soil during seismic loading. The solution is based on the seismic coefficient method and velocity field method from the upper bound theorem. The solution was verified by a series of experiments. It was found that the results in the case of severe seismic loading, most of the available solutions are over-estimating the bearing capacity.

A large-scale model was performed with five series of tests consisting of (40 models) of shear wall foundations to study the nonlinear load-deformation behaviour during cyclic and seismic loading [9]. The parameters that were systematically studied were footing dimensions, depth of embedment of footing, wall weight, and initial static vertical factor of safety, unit weight of soil, and soil type (dry sand and saturated clay). It was found that there is a reduction in stiffness of which may be due to the deformed shape of the

foundation–soil interface and uplift associated with large rotations. Moreover, it was concluded that the permanent settlement beneath the foundation continue to accumulate with the number of cycles of loads, though the rate of accumulation of settlement decreases as the foundation embeds.

The effect of ground inclination and embedment depth for footing subjected to earthquake excitation was studied [10]. It was found that the bearing capacity factors (N_c and $N_{\gamma q}$) decreased with an increase in kh (values of seismic acceleration coefficient). Unlike most of the results reported in the literature for the seismic case, the computational results take into account the shear resistance of soil mass above the footing level. An increase in the depth of the embedment leads to an increase in the magnitudes of both N_c and $N_{\gamma q}$.

The inertia loads in the ground and beneath the footings reducing the bearing capacity of the footing when subjected vertical loading. These results cannot be applied for seismic bearing capacity of shallow footing due to the transient nature of the seismic loading as compared to the sustained nature of static loads. This technical note appears in the bearing capacity calculation given in Part 5 of Euro code 8, which declares that shallow footing bearing strength for cohesive soils is not sensitive to the seismic horizontal acceleration, but dry cohesionless soil may be more sensitive [11].

Experimental and numerical studies for the effect of harmonic dynamic loading on a shallow foundation of different sizes and depth of embedment in dry and saturated sand with different relative density was performed [12]. It was found that displacement amplitude for dry dense sand is less than of dry loose sand. They showed that for foundation rested at the surface, the ratio of displacement amplitude between dense sand to loose sand varying from (0.27 to 1.00) and (0.03 to 0.94) for footing dimensions (100×200 mm) and (200×400 mm), respectively. At the same time, the ratio for the embedded footing becomes (0.24 to 0.99) and (0.10 to 0.97) for the footing dimensions (100×200 mm) and (200×400 mm), respectively. These results are attributed to the increase of soil stiffness in the dense state that makes the soil stiffer and resist vibrations as well as it can be due to trench and sidewall effects when embedded.

The mechanical property of soil and reaction of forced vibration is responsible to the behaviour of frequency and propagation of the dynamic waves. They convert the periodic motion of input to the nonlinear loading. The liquefaction with high magnitude occurs in the deep of soil foundation, as well as the pore water pressure magnitude reduces near the surface, this fluctuation of pore water pressure causes differential settlement. There is no direct effect of frequency on the differential settlement, during which soil is under the

liquefied state [13]. Same observations were noticed by Fattah et al. [14] for machine foundations.

Moghaddas Tafreshi et al. [15] stated that the results of plate load tests that imposed incremental cyclic loading to a sandy soil bed containing multiple layers of granulated rubber-soil mixture (RSM) at large model scale when the thickness of the RSM layer is smaller, or larger, settlements increase and, at large thicknesses may even exceed those of untreated soil. Layers of the RSM reduced the vertical stress transferred through the foundation depth by distributing the load over a wider area. With the inclusion of RSM layers, the coefficient of elastic uniform compression decreases by a factor of around 3-4. A softer response was obtained when more RSM layers were included beneath the footing damping capacity improves appreciably when the sand bed incorporates RSM layers. Numerical modelling using "FLAC-3D" confirms that multiple RSM layers will improve the performance of a foundation under heavy loading.

The effect of near-fault ground motion on a timber beam was investigated with reference to small displacement theory [16]. The simulated near-fault ground motion is applied to the fixed base of a timber frame model. The beam is placed in a single span of a timber frame. The beam has two different length sizes of 1.8 and 3.3 meters. The seismic load-displacement, seismic load-strain, and strain-displacement was calculated for all models. The beam was modelled as a nonlinear analysis. The numerical analysis results indicate that the inertial interaction, energy dissipation, and nonlinear deformation of beams in timber frames have directly related with frame span. In beams with a smaller length, higher seismic loading caused lower displacement. Also, the displacement was reduced by reducing the length of the beam. The inertial interaction, energy dissipation, and nonlinear deformation were changed with respect to the length of the beam.

The purpose of this research is to determine the vertical and lateral displacement under the influence of the earthquake. In addition, it is required to know the influence of the soil layer on the impact of the earthquake on the displacement and the effect of changing the stiffness ratio of soil to the footing on the value of lateral and vertical displacement. The adopted technique of numerical analysis by using Abaqus is of great interest to improve the seismic behaviour of soil foundation system under the earthquake excitation.

2. EARTHQUAKE LOADING

Figure 1 shows the time history for the El Centro earthquake which is applied to the model of the foundation-soil system that would built in the Abaqus program.

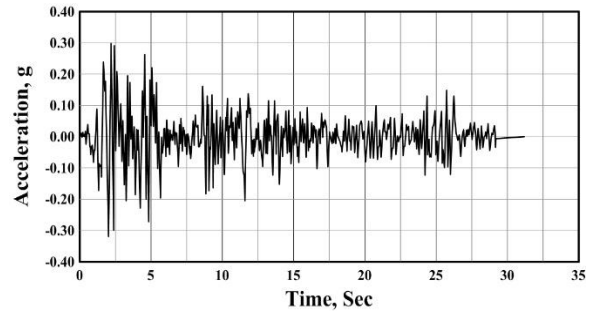


Figure 1. Time-history of acceleration of the El Centro earthquake

In order to obtain the accuracy of the program, the model was built by using the Abaqus program in this research and then the model was verified with the results of the ultimate bearing capacity of the foundation under seismic centred load N_{max} as given in Equation (1). The results of the verification are shown in Table 1.

$$N_{max} = \frac{1}{2} \rho g (1 \pm \frac{av}{g}) B 2N\gamma \quad (1)$$

where:

g : acceleration of gravity;

av : vertical ground acceleration, that may be taken as being equal to $0.5 ag$. S ;

$N\gamma$: Bearing capacity factor.

S : Soil factor defined in EN 1998 – 1:2004

The dimensionless soil inertia force F is obtained by Equation (2):

$$F = \frac{ag}{g \tan(\phi'd)} \quad (2)$$

where: $\phi'd$: Design angle of the shearing resistance of soil.

For cohesionless soils, inertia forces may be neglected if $ag.S < 0.1g$.

3. FAILURE CRITERIA

Strain levels are produced in the ground with different magnitudes. If strains below the order of 10^{-5} , the deflection of soils is elastic and recoverable, the small strains would be small amplitude vibration or wave propagation through the ground. The strain between (10^{-4} and 10^{-2}), the behaviour of soils is elastic-plastic and produces irrecoverable permanent deflections [17]. This criterion will be followed in this research.

4. MODEL CONFIGURATION

The models of soil-foundation system were implemented in the Abaqus program as two parts, one

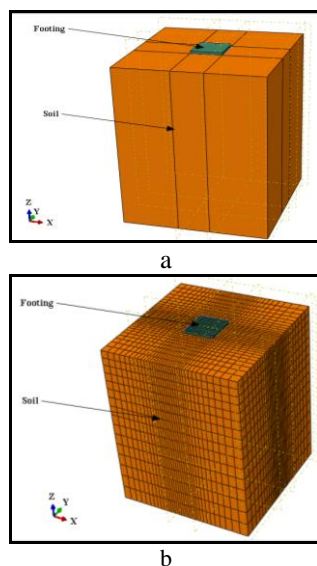
TABLE 1. Results of Verification of model

Method	Parameters						
	B	ρ	g	αv	S	$N\gamma$	Nmax
Ultimate bearing capacity of the foundation under seismic vertical load	14	1.55	9.81	1.99	1.35	9.7	17343.5
Finite element using Abaqus	14	1.55	9.81	----	----	----	16212.3

of them is the shallow foundation with dimensions of (14 m \times 14 m) and the thickness taken as (0.5, 1.0 and 2.0 m) while the other part is the soil media with dimensions of (60 m \times 60 m) and the depth of soil was 10, 20 and 40 m. Figure 2 shows the two parts of the footing and the soil domain after the assembly. The interaction of the base footing and the top surface of the soil is activated to be of type normal behaviour hard contact. Parameters that would be addressed in this research is summarized in Table 2.

5. MATERIAL PROPERTIES OF THE MODEL

As previously explained, the model consists of two parts, one of them is the footing and the other is soil. For the purpose of distinguishing each part from the other, the properties of the materials were defined

**Figure 2.** The assembly and mesh of footing and soil**TABLE 2.** The parametric study

Model	Parameter			
	Width of footing, b (m)	Thickness of footing, t (m)	Thickness (depth) of soil layer, d (m)	Stiffness ratio (Es/Ec)
Model 1	14	0.5	10	0.68
Model 2	14	0.5	20	0.68
Model 3	14	0.5	40	0.68
Model 4	14	1	10	0.68
Model 5	14	1	20	0.68
Model 6	14	1	40	0.68
Model 7	14	2	10	0.68
Model 8	14	2	20	0.68
Model 9	14	2	40	0.68
Model 10	14	2	10	0.85
Model 11	14	2	10	1.0
Model 12	14	2	10	1.7

including the footing concrete materials which follows linear elastic behaviour. For soil, Jefferies and Been [6] stated that the soil is the best modelled as plastic materials when subjected to earthquake loading of high level of strain resulting from the high magnitude of energy of such loading. Hence, the soil is represented by extended Drucker-Prager family of plasticity model which is the best suited for the behaviour of granular soils in which the yield behaviour related to the equivalent pressure stress. The inelastic behaviour may be associated with frictional mechanisms such as sliding of particles across each other. Tables 3 and 4 show the properties of the materials for both footing and sand.

TABLE 3. Properties of concrete footing

Property	Value
Unit weight, γ_c (kN/m ³)	24
Elastic modulus, E_c (kN/m ²)	23500
Poisson's ratio, ν	0.15

TABLE 4. Properties of sand soil

Property	Value
Angle of friction, ϕ	32
Flow stress ratio	1
Dilation angle, ψ	3
Poisson's ratio, ν	0.25
Modulus of deformation, E_s (kN/m ²)	16000
Dry unit weight of soil, γ_d (kN/m ³)	15.5

6. DEFINITION OF LOADING AND BOUNDARY CONDITIONS

In this section, the earthquake loading explained in section 2, is applied at the base of the soil model towards the base of the footing. The application of loading and the boundary conditions are defined as shown in Figure 3, whereas displacements are allowed in horizontal and vertical directions for lateral boundaries.

6. RESULTS AND DISCUSSION

Figures 4 to 6 show the vertical displacement-time history response generated due to earthquake loading of the model. It can be noticed in general that, as the duration of earthquake increases, the vertical displacement of the footing increases. This behaviour can be attributed to the loose state of soil prior to the application of the earthquake loading and when the earthquake loading is applied, the state of the soil changes from loose to dense. As a result of continuous earthquakes, the soil state changes from dense to loose by dilation which results in high displacement in the footing. Clearly, it can be illustrated from the figures

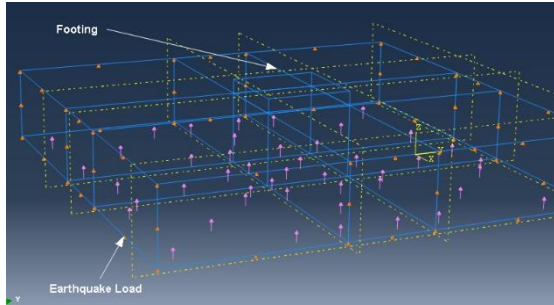


Figure 3. The applied earthquake load in the model

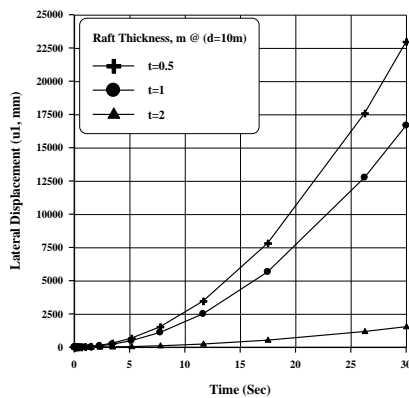


Figure 4. Lateral displacement with time for footings with different thicknesses placed on soil layer of depth (d=10 m) below the footing

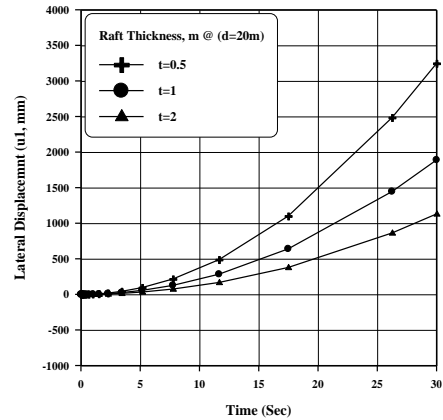


Figure 5. Lateral displacement with time for footings with different thicknesses placed on soil layer of depth (d=20 m) below the footing

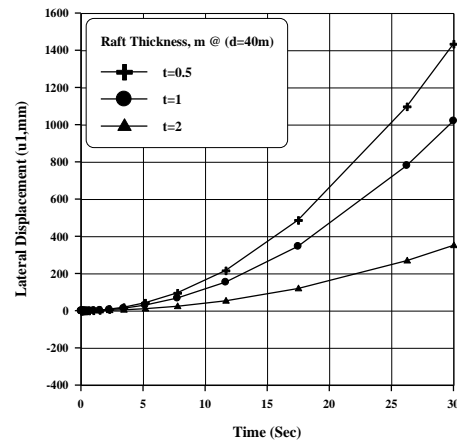


Figure 6. Lateral displacement with time for footings with different thicknesses placed on soil layer of depth (d=40 m) below the footing

that with an increase of the soil layer thickness below the footing, the vertical displacement decreases. In addition, the vertical displacement decreases from (80, 12, and 2 mm) when the distance between the footing and the point of influence of the earthquake loading varies from (10, 20, and 40 m), respectively. It was expected that the highest value of vertical displacement incidence with the highest value of the earthquake loading but the results revealed that there is a time lag of about 0.27 s.

Figure 7 shows the calculated vertical displacement versus the distance between the footing and the point of influence of the earthquake, it can be noticed that there is no apparent effect of the footing thickness on the vertical displacement because the direction of the earthquake load is perpendicular to the base of the foundation and an increase in the distance between the footing and the point of influence of the earthquake loading leads to decrease in the vertical displacement.

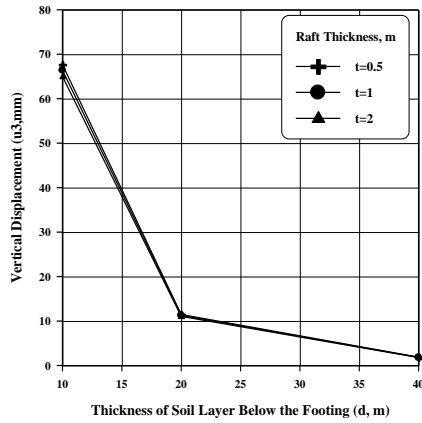


Figure 7. Vertical displacement versus soil layer thickness below the footing

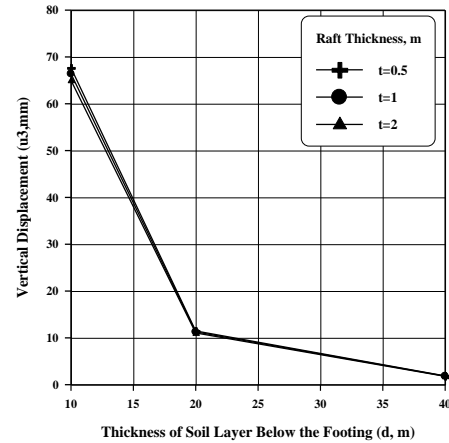


Figure 8. Lateral displacement versus soil layer thickness below the footing

Figure 8 illustrates variations of the calculated lateral displacement with the distance between the footing and the point of influence of the earthquake. It can be noticed that the greater the distance between the footing and the point of influence of earthquake load, the greater the effect of damping to the earthquake load and consequently decrease in lateral displacement as well as the depth of soil layer is great, the length of the wave increase that cause more attenuation during earthquake. The effect of damping appears clearly when the depth of soil is 40 m.

The effect of soil stiffness on the vertical and lateral displacement of the footing was elaborated by changing soil stiffness several times with keeping footing stiffness constant. Figures 9 and 10 show the vertical and lateral displacement response with respect to time at different values of stiffness ratio (E_s/E_c), where E_c is the modulus of elasticity of concrete and E_s is the modulus of elasticity of soil. In general, an increase of the stiffness ratio value (E_s/E_c) leads to a decrease in the vertical displacement of the footing. The vertical displacement decreases from (65, 52, 44, and 26 mm) when the stiffness ratio increases from (0.68, 0.85, 1, and 1.7), respectively. On the other hand, the response of the lateral displacement decreases with an increase in the value of stiffness ratio until reach the value of ($E_s/E_c = 1$).

It can be noticed that the lateral displacement starts to increase with an increase in the value of stiffness ratio, this is attributed to the state of the soil which has changed from loose to dense that leads to and facilitate the rapid transmission of the shockwave. The lateral displacement decreases from (1538, 1303, and 744 mm) when the value of stiffness ratio increases from (0.68, 0.85, and 1.00), respectively.

The shape of the model after completing the analysis and the deformation that occurred for the models due to the shockwave loading can be seen in Figure 11.

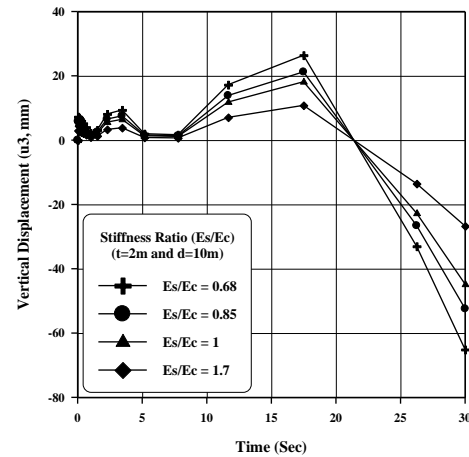


Figure 9. Vertical displacement with time for footings of different stiffness ratios ($t = 2.0$ m and $d = 10$ m)

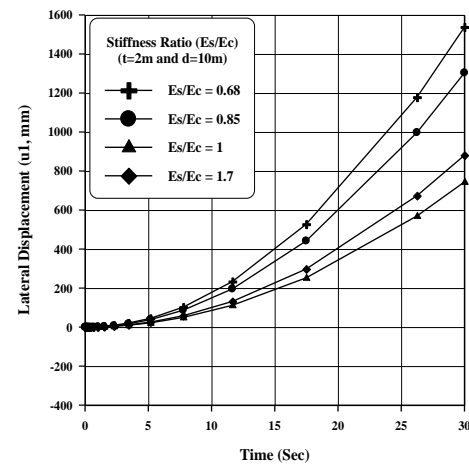


Figure 10. Lateral displacement with time for footings of different stiffness ratios ($t = 2.0$ m and $d = 10$ m)

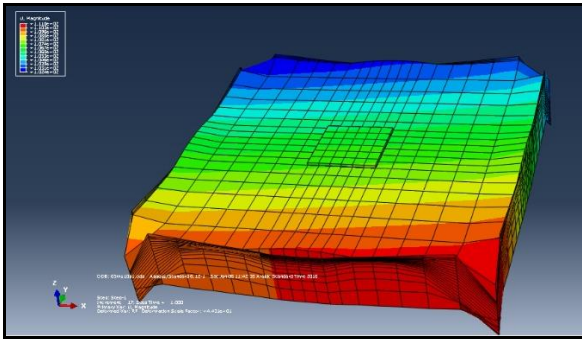


Figure 11. The deformed shape of deflection when ($t= 0.5$ m and the soil layer thickness below the footing, $d=10$ m)

7. CONCLUSIONS

From the discussions carried out in this work and other observations made during the numerical analyses, the following conclusions are made.

- As the time of applied earthquake increases, the vertical displacement of the footing increases.
- The vertical and lateral displacement increase with an increase in the depth of soil layer below the footing.
- The time lag between the maximum vertical displacement and the highest value of the earthquake loading is about (0.27 s).
- An increase in the thickness of the footing lead to a decrease in lateral displacement of the footing, while there is no obvious effect of the footing thickness on the vertical displacement since the direction of the earthquake load is perpendicular to the base of the footing.
- An increases in the depth of the soil layer below the footing lead to an increase in the attenuation of the earthquake load and consequently to decrease in lateral displacement.
- An increase in the stiffness ratio value (E_s/E_c) leads to a decrease in the vertical displacement. The response of the lateral displacement decreases with an increase in the value of stiffness ratio until the value of ($E_s/E_c = 1$). The lateral displacement starts to increase with an increase in the value of stiffness ratio.

8. REFERENCES

1. Ishihara, K. and Koga, Y., "Case studies of liquefaction in the 1964 niigata earthquake", *Soils and Foundations*, Vol. 21, No. 3, (1981), 35-52. doi:10.3208/sandf1972.21.3_35
2. Moura, A., Neto, S. and de Aguiar, M., "A comparative study of vibration frequency estimates of the surface foundations of wind turbines built on the sand dunes of the ceará coast", (2008).
3. Das, B.M. and Luo, Z., "Principles of soil dynamics, Cengage Learning, (2016).
4. Richart, F.E., "Foundation vibrations", *Transactions of the American Society of Civil Engineers*, Vol. 127, No. 1, (1962), 863-897.
5. Jefferies, M. and Been, K., "Soil liquefaction: A critical state approach, CRC press, (2015).
6. Roy, D., "Design of shallow and deep foundations for earthquakes", *J. Geotech. Earthq. Eng.* (2013), 1-8.
7. Tiznado, J.C. and Paillao, D., "Analysis of the seismic bearing capacity of shallow foundations", (2014). doi.org/10.4067/S0718-915X2014000200005
8. Maeda, Y., Irie, T. and Yokota, Y., "Bearing capacity formula for shallow foundations during earthquake", in 13th world conference on earthquake engineering. Vancouver, BC. 1-6.
9. Gajan, S., Kutter, B.L., Phalen, J.D., Hutchinson, T.C. and Martin, G.R., "Centrifuge modeling of load-deformation behavior of rocking shallow foundations", *Soil Dynamics and Earthquake Engineering*, Vol. 25, No. 7-10, (2005), 773-783. doi:10.1016/j.soildyn.2004.11.019
10. Chakraborty, D. and Kumar, J., "Seismic bearing capacity of shallow embedded foundations on a sloping ground surface", *International Journal of Geomechanics*, Vol. 15, No. 1, (2015), 04014035. doi:10.1061/(ASCE)GM.1943-5622.0000403
11. Pender, M., "Earthquake inertia effects on shallow foundation bearing strength", *Geotechnique*, Vol. 68, No. 7, (2018), 640-645. doi:10.1680/jgeot.17.T.006
12. Fattah, M.Y., Al-Mosawi, M.J. and Al-Ameri, A.F., "Dynamic response of saturated soil-foundation system acted upon by vibration", *Journal of Earthquake Engineering*, Vol. 21, No. 7, (2017), 1158-1188. doi:10.1080/13632469.2016.1210060
13. Namdar, A., "Liquefaction zone and differential settlement of cohesionless soil subjected to dynamic loading", *Electronic Journal of Geotechnical Engineering*, Vol. 21, (2016), 593-605.
14. Fattah, M.Y., Al-Mosawi, M.J. and Al-Ameri, A.F., "Stresses and pore water pressure induced by machine foundation on saturated sand", *Ocean Engineering*, Vol. 146, (2017), 268-281. doi:10.1016/j.oceaneng.2017.09.055
15. Moghaddas Tafreshi, S., Darabi, J. and Dawson, A., "Cyclic loading response of footing on multi-layered rubber-soil mixtures", *Geomechanics and Engineering*, Vol. 14, No. 2, (2020). doi:10.12989/gae.2018.14.2.115
16. Namdar, A., Dong, Y. and Liu, Y., "Timber beam seismic design—a numerical simulation", *Frattura ed Integrità Strutturale*, Vol. 13, No. 47, (2019), 451-458. doi:10.3221/IGF-ESIS.47.35
17. Daghigh, Y., "Numerical simulation of dynamic behaviour of an earthdam during seismic loading", (1993).

Persian Abstract

چکیده

هنگام زلزله بنیاد ساختمانها و سازه ها با خطراتی مواجه هستند و منجر به جابجایی های زیاد می شوند که می تواند باعث خرابی سازه ها شود. این تحقیق به صورت عددی اثر زلزله را بر جابجایی عمودی و جانبی پی های در حال سکون در خاک توضیح می دهد. ضخامت پی و عمق لایه خاک زیر پی به ترتیب (۰.۵، ۱.۰ و ۲.۰ متر) و (۱۰، ۲۰ و ۴۰ m) در نظر گرفته شد. همچنین نسبت سختی خاک به پایه نیز در ۰/۳۸، ۰/۸، ۱.۰ و ۱.۷ بیان شده است. نتایج نشان می دهد با افزایش مدت زمان وقوع زلزله، افزایش جابجایی عمودی در پی را نشان می دهد. افزایش ضخامت لایه خاک زیر پی منجر به کاهش جابجایی عمودی و جانبی می شود. در حالی که افزایش ضخامت پی منجر به کاهش جابجایی جانبی پی می شود، در عین حال هیچ تأثیری در جابجایی عمودی مشاهده نشده است. مشاهده شد که فاصله زمانی بین حداکثر جابجایی عمودی و بیشترین مقدار بارگذاری زلزله حدود ۰.۲۷ ثانیه است. مشخص شد که با افزایش فاصله بین پی و منبع بار زلزله، در حالی که جابجایی جانبی کاهش می یابد، تأثیر میرایی بر بار زلزله افزایش می یابد. نتایج نشان داد که افزایش نسبت سفتی منجر به کاهش جابجایی عمودی و کاهش پاسخ جابجایی جانبی تا رسیدن به ارزش سختی قریب به یک می شود.
